



HF  
16,6

# 3D unsteady RANS simulation of turbulent flow over bluff body by non-linear model

660

V. Ramesh, S. Vengadesan and J.L. Narasimhan

*Department of Applied Mechanics, IIT Madras, Chennai, India*

Received February 2005  
Revised December 2005  
Accepted December 2005

## Abstract

**Purpose** – To perform 3D unsteady Reynolds Averaged Navier-Stokes (URANS) simulations to predict turbulent flow over bluff body.

**Design/methodology/approach** – Turbulence closure is achieved through a non-linear  $k - \epsilon$  model. This model is incorporated in commercial FLUENT software, through user defined functions (UDF).

**Findings** – The study shows that the present URANS with standard wall functions predicts all the major unsteady phenomena, with a good improvement over other URANS reported so far, which incorporate linear eddy viscosity models. The results are also comparable with those obtained by LES for the same test case.

**Originality/value** – When comparing the computational time required by the present model and by LES, the accuracy achieved is significant and can be used for simulating 3D unsteady complex engineering flows with reasonable success.

**Keywords** Turbulence, Simulation, Turbulent flow, Differential equations

**Paper type** Research paper

## 1. Introduction

The incompressible turbulent flow around bluff bodies is of much interest due to their frequent engineering and scientific applications, such as design of tower structures, suspension bridges, chimney stacks, tall buildings, etc. The complex phenomena involve streamline curvature, separation and formation of large unsteady vortical structures. In numerical simulation, treatment of turbulence is crucial in predicting the complex behavior of such flows. Simulation of engineering turbulent flows is either done by statistical modeling of turbulence based on the Reynolds-Averaged Navier-Stokes (RANS) equations or by large eddy simulation (LES), where the equations are spatially filtered and subgrid-scale stress terms are modeled. In particular, when the flow is not statistically stationary, Reynolds averaging is not same as the time-averaging and so the simulation must be a time dependent one. This significantly increases the computational time over conventional RANS. Recently, Nakayama and Miyashita (2001) and Iaccarino *et al.* (2003) demonstrated the improvement in prediction by unsteady RANS (URANS) over that by steady RANS. Rodi (2000) reported in ECCOMAS 2000 that solving RANS with statistical turbulence model plays an important role, since LES is still in development stages for high Reynolds number flows. The emphasis was laid more on developing nonlinear eddy viscosity models (EVMS) rather than going for simple linear EVMs or numerically more troublesome Reynolds stress models (RSM).



Earlier, nonlinear EVMs were proposed by Gatski and Speziale (1993), Craft *et al.* (1996) and Shih *et al.* (1997). The former derived the constants from RSM and the model is referred as explicit algebraic stress model (EASM). This model is found to be numerically very stiff. The latter two studies tuned the coefficients based on rapid distortion theory and applying realizability constraints for the Reynolds stresses resulting due to high strain rates. These models were mostly applied to internal flows. Besides, all these nonlinear EVMs are low Reynolds number models, for which near-wall resolution must be as low as  $y^+ < 1$  and hence mostly used for 2D simulation only. Requirement of computational resources becomes very high when they are applied to external flows and also when solving time dependent flows. Durbin (1995) developed  $v^2 - f$  model, which is also a reduced form of RSM. Here, an equation for Reynolds stress  $v^2$  and a Helmholtz elliptical equation for  $f$  (the term  $-kf$  is the production term in transport equation for  $v^2$ ) are solved along with transport equations for  $k$  and  $\varepsilon$ . This model also requires very high near-wall resolution apart from solving the four additional equations. Recently, Kimura and Hosoda (2003) proposed a non-linear model. The coefficients were obtained for flow around bluff bodies. The requirement for very high resolution near the wall is avoided by a wall function approach. This decreased the overall mesh size substantially and thus reducing computational time, even when solving a 3D time dependent flow.

In the present work, unsteady 3D RANS computations are performed by adopting a non-linear  $k - \varepsilon$  model as turbulence closure. The test case considered is flow around a square cylinder at Reynolds number based on cylinder width and incoming velocity of  $Re = 22,000$ . This test case is a standard benchmark case and experimental data of Lyn *et al.* (1995) is considered. The time averaged quantities and bulk parameters obtained by the present simulation are compared with RANS simulations done earlier by Franke and Rodi (1991) (hereafter referred to as FR 1991) and with LES data of Nakayama and Vengadesan (2002) (hereafter referred to as NV 2002).

## 2. Computational method

### 2.1 Basic equations

The ensemble averaged RANS equations for an incompressible and isothermal flow are continuity equation:

$$\frac{\partial U_i}{\partial x_i} = 0 \quad (1)$$

Momentum equation:

$$\frac{\partial U_i}{\partial t} + \frac{\partial U_j U_i}{\partial x_j} = g_i - \frac{1}{\rho} \frac{\partial p}{\partial x_i} + \frac{\partial(-\overline{u_i u_j})}{\partial x_j} + \nu \frac{\partial^2 U_i}{\partial x_j^2} \quad (2)$$

where  $x_i$  is the spatial co-ordinate,  $t$  is the time,  $U_i$  is the averaged velocity,  $u_i$  is the fluctuating velocity,  $p$  is the averaged pressure and  $\rho$  is the fluid density. Owing to ensemble averaging process, further unknowns are introduced to the momentum equations by means of Reynolds stresses  $(-\overline{u_i u_j})$ . In engineering flows, closure approximation using two-equation models (EVMs) for  $-\overline{u_i u_j}$  have gained popularity due to their simplicity. In this paper, the study is confined to  $k - \varepsilon$  models, which employ additional transport equations for turbulent kinetic energy  $k$  and its dissipation rate  $\varepsilon$ .

Transport equations for  $k$  and  $\varepsilon$  are given as:

$$\frac{\partial k}{\partial t} + \frac{\partial k U_j}{\partial x_j} = -\overline{u_i u_j} \frac{\partial U_i}{\partial x_j} - \varepsilon + \frac{\partial}{\partial x_j} \left\{ \left( \frac{\nu_t}{\sigma_k} + \nu \right) \frac{\partial k}{\partial x_j} \right\} \quad (3)$$

$$\frac{\partial \varepsilon}{\partial t} + \frac{\partial \varepsilon U_j}{\partial x_j} = -C_{\varepsilon 1} \frac{\varepsilon}{k} \overline{u_i u_j} \frac{\partial U_i}{\partial x_j} - C_{\varepsilon 2} \frac{\varepsilon^2}{k} + \frac{\partial}{\partial x_j} \left\{ \left( \frac{\nu_t}{\sigma_\varepsilon} + \nu \right) \frac{\partial \varepsilon}{\partial x_j} \right\} \quad (4)$$

where  $k$  is the turbulent kinetic energy,  $\varepsilon$  is the turbulent kinetic energy dissipation rate,  $\nu_t$  is the eddy viscosity and  $\nu$  is molecular kinematic viscosity.

### 2.2 The non-linear $k - \varepsilon$ model

In the standard  $k - \varepsilon$  model, the Reynolds stresses are calculated by the linear relation proposed by Boussinesq as:

$$-\overline{u_i u_j} = \nu_t S_{ij} - \frac{2}{3} k \delta_{ij} \quad (5)$$

It is well known that the standard  $k - \varepsilon$  model does not take into account the anisotropic effects and fails to represent the complex interaction mechanisms between Reynolds-stresses and mean velocity field. For example, the linear model fails to mimic the effects related to streamline curvature or secondary motion. These anisotropic effects can be predicted by introducing non-linear expression for the Reynolds stresses as given in the following expression:

$$-\overline{u_i u_j} = \nu_t S_{ij} - \frac{2}{3} k \delta_{ij} + \left( \left( -\frac{k}{\varepsilon} \nu_t \right) \times \text{non-linear terms} \right) \quad (6)$$

Constitutive relations for the Reynolds stresses in general form as given in the expression below have been proposed by Gatski and Speziale (1993), Craft *et al.* (1996), Shih *et al.* (1997) and Kimura and Hosoda (2003). Coefficients ( $\alpha_i$ ,  $i = 1$  to 7) in these non-linear terms should be carefully determined because they are expected to influence the accuracy and performance of the model:

$$\begin{aligned} & \alpha_1 (S_{il} \Omega_{lj} + \Omega_{il} S_{lj}) + \alpha_2 \left( S_{il} S_{lj} - \frac{1}{3} S_{km} S_{mk} \delta_{ij} \right) + \alpha_3 \left( \Omega_{il} \Omega_{lj} - \frac{1}{3} \Omega_{km} \Omega_{mk} \delta_{ij} \right) \\ & + \alpha_4 \frac{k}{\varepsilon} (S_{kl} \Omega_{lj} + S_{kj} \Omega_{li}) S_{kl} + \alpha_5 \frac{k}{\varepsilon} \left( \Omega_{il} \Omega_{lm} S_{mj} + S_{il} \Omega_{lm} \Omega_{mj} + \frac{2}{3} S_{lm} \Omega_{mn} \Omega_{nl} \delta_{ij} \right) \\ & + \alpha_6 \frac{k}{\varepsilon} (S_{il} S_{kl} S_{kl}) + \alpha_7 \frac{k}{\varepsilon} (S_{ij} \Omega_{kl} \Omega_{kl}) \end{aligned}$$

As mentioned earlier in the introduction, these coefficients are determined through rapid distortion theory and realizability principle. In the present study, the non-linear coefficients considered are those proposed by Kimura and Hosoda (2003) for bluff body flows. In this model, previous experimental data are also considered for evaluating these coefficients. These are given as:

$$\alpha_1 = \frac{(C_3 - C_1)}{4.0}; \quad \alpha_2 = \frac{(C_1 + C_2 + C_3)}{4.0}; \quad \alpha_3 = \frac{(C_2 - C_1 - C_3)}{4.0};$$

$$\alpha_4 = 0.02f_M(M); \quad \alpha_5 = 0; \quad \alpha_6 = 0; \quad \alpha_7 = 0$$

where  $C_1 = 0.4f_M(M)$ ,  $C_2 = 0$ ,  $C_3 = -0.13f_M(M)$  and  $f_M(M) = (1 + 0.01M^2)^{-1}$ ,

$$M = \max(S, \Omega), \quad S = \frac{k}{\varepsilon} \sqrt{\frac{1}{2} \left( \frac{\partial U_i}{\partial x_j} + \frac{\partial U_j}{\partial x_i} \right)^2}, \quad \Omega = \frac{k}{\varepsilon} \sqrt{\frac{1}{2} \left( \frac{\partial U_i}{\partial x_j} - \frac{\partial U_j}{\partial x_i} \right)^2}$$

$S$  is the strain parameter and  $\Omega$  is the rotation parameter. In RANS models, the turbulent viscosity  $\nu_t$  is given by the expression  $\nu_t = C_\mu k^2 / \varepsilon$  and in standard  $k - \varepsilon$  model  $C_\mu$  is set to a constant value of 0.09. It is known that this constant value does not satisfy realizability constraint. In the present model,  $C_\mu$  is expressed as a function of  $S$  and  $\Omega$  and is given by:

$$C_\mu = \min \left( 0.09, \frac{0.3}{1 + 0.09M^2} \right) \quad (7)$$

### 3. Test case and numerical strategies

A commercial package FLUENT 6.1 has been used to solve the basic governing equations for velocities and turbulent quantities. The equations are discretized using the finite volume method on a collocated grid in fully implicit form. The second order upwind differencing scheme is used for convective terms and also the terms in equations for turbulent quantities,  $k$  and  $\varepsilon$ . Central differencing scheme is adopted for solving diffusion terms. The second order implicit scheme was used for time integration of each equation. The SIMPLE algorithm was used for coupling the pressure and velocity terms. The present non-linear model is incorporated in FLUENT through user-defined functions (UDFs). The non-linear stress term is added as source term in equations for  $k$  and  $\varepsilon$ . The turbulent viscosity is also made to vary according to equation (7) through UDFs.

In the present work, the turbulent flow past a square cylinder is simulated. This test case is considered as one of the benchmark problems in simulations. The flow separation is fixed at the front corners. There is a periodic vortex shedding in the wake due to the separated shear layers. Many numerical works have been done and experimental data are also available for this flow. Franke and Rodi (1991) have simulated the flow around a square cylinder using RANS equations (standard  $k - \varepsilon$  two-layer) and RSM model. Rodi (1997) compared different unsteady RANS turbulence models (standard  $k - \varepsilon$  Kato-Launder modification and two-layer approach) and LES for the case of flow past a square cylinder. LES has also been performed by Murakami and Mochida (1995) and NV 2002. These numerical simulations are performed for comparison with the experimental data of Lyn *et al.* (1995) which was carried out at  $Re = 22,000$ .

In the present work, we take the same test case and perform unsteady 3D RANS computation by non-linear  $k - \varepsilon$  model. The results using the present model are compared with the experimental data of Lyn *et al.* (1995) and with other numerical

results obtained using RANS and LES. The schematic representation of the computational domain is shown in Figure 1. Structured grid in Cartesian coordinates is chosen, where  $x$ -axis is along the streamwise direction,  $y$ -axis is in the cross-stream direction and  $z$ -axis is in the spanwise direction, respectively, as shown in the figure. The present model is a high Reynolds number model and hence the first grid point is placed outside the viscous sub-layer. Two grid arrangements have been tried. In one grid, the first grid point is placed at a distance of  $\delta y = 0.01D$  from the wall and in another grid, it is placed at  $0.05D$  from the wall. Grids are non-uniformly placed in both  $x$ - and  $y$ -directions and uniformly spaced in the  $z$ -direction. Total mesh sizes are  $153 \times 120 \times 32$  and  $120 \times 70 \times 40$ .

Boundary conditions are specified at boundary locations. At inlet, a uniform velocity  $U_o = 8.34 \text{ m/s}$  and turbulence intensity,  $I = 2$  percent as observed in the experiment are prescribed. Convective boundary condition is given at the outlet. Symmetry boundary condition is forced at the cross-stream direction. Periodic boundary conditions are applied at the top and bottom (spanwise) boundaries. Standard wall functions of Launder and Spalding (1974) are used here to bridge the viscosity affected near wall region and the fully turbulent outer region. Calculations are advanced with an increment of  $dt = 1.0 \times 10^{-3} \text{ s}$ . The solution is started and allowed

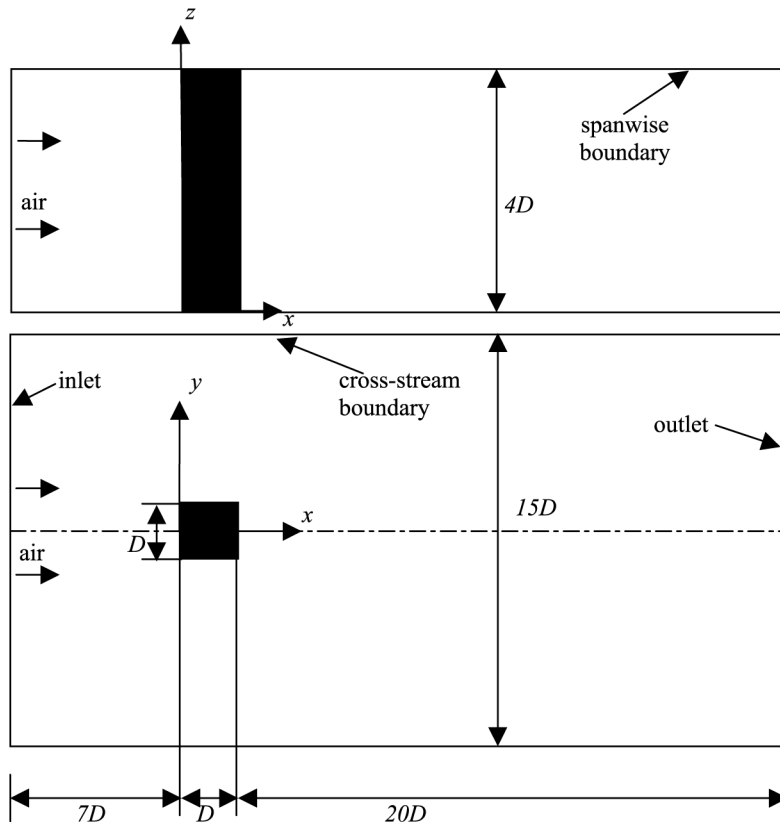


**Figure 1.**  
Schematic representation  
of the computational  
domain

to march in time until the vortex shedding becomes periodic. This is observed from the variation of lift coefficient as a function of time as shown in Figure 2. Once the flow becomes periodic, mean quantities are obtained by averaging the instantaneous quantities for over ten vortex shedding cycles.

Streamwise velocity distributions at various locations on the side surface predicted by both grids are shown in Figure 3. It can be observed that results from both grids are close to each other. The bulk parameters obtained by both grids are given in Table I. Hence, further results are presented for the grid size  $153 \times 120 \times 32$  with  $\delta y = 0.01$ .

#### 4. Results and discussion

The flow around a square cylinder computed by the present model at  $Re = 22,000$  produced coherent vortex shedding. Iso-vorticity contours at different instances of a vortex shedding cycle are shown in Figure 4. Computations by Franke and Rodi (1991), where the standard  $k - \varepsilon$  model in conjunction with wall functions was used arrived at a steady solution and thus no vortex-shedding. The time-averaged streamwise velocity component along the centerline of the square cylinder is shown in Figure 5. As it can be observed from the figure, the  $k - \varepsilon$  models predicted very large recirculation zone and the recovery to free stream velocity is very slow, the present NLKE model and LES predict the same trend of attaining the free stream velocity, as reported in the experiment. The RSM attains the free stream velocity much faster than all other models and also under-predicts the reattachment point. The bulk parameters of interest like the reattachment length ( $x_r/D$ ), mean drag ( $C_{d, \text{mean}}$ ), fluctuating drag ( $C_{d, \text{rms}}$ ), mean lift ( $C_{l, \text{mean}}$ ) fluctuating lift ( $C_{l, \text{rms}}$ ), Strouhal number ( $St$ ), obtained by present computations and by different models are presented in the Table II. As it can be

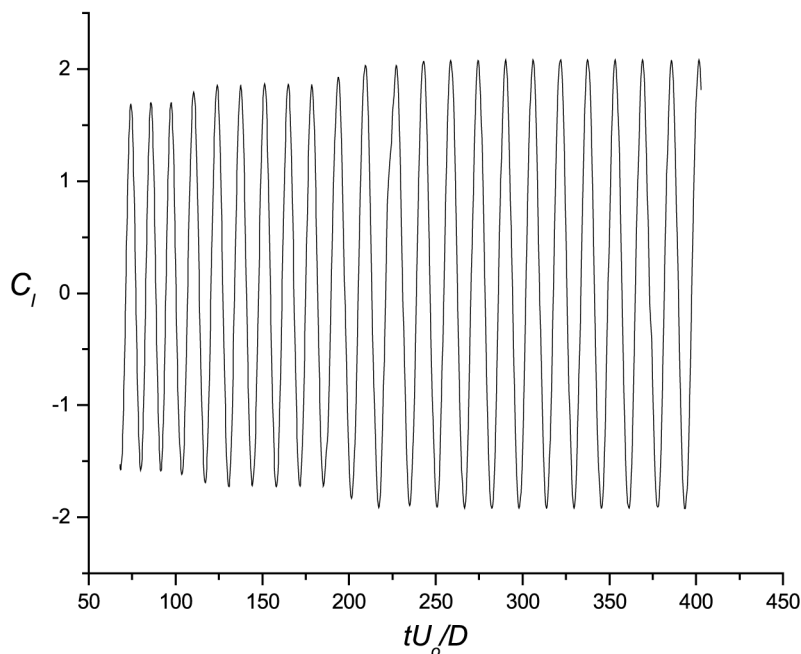


**Figure 2.**  
Variation of lift coefficient  
with time

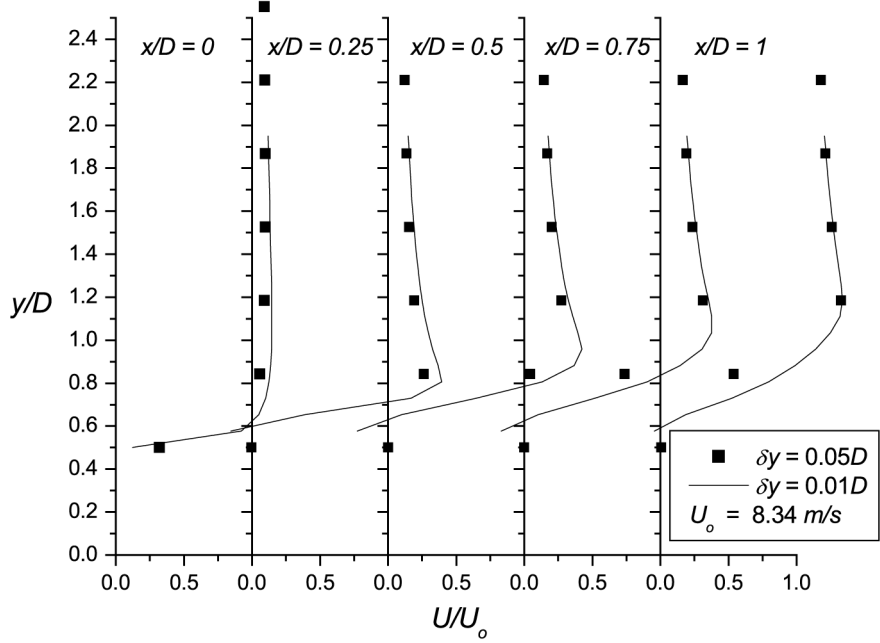


**Figure 3.**  
Mean velocity plots on the side surface of the cylinder

Parameter	Grid 1	Grid 2
$\delta y$	0.05D	0.01D
$\hat{C}_{d, \text{mean}}$	1.64	1.899
$C_{d, \text{rms}}$	0.06	0.0817
$\hat{C}_{l, \text{mean}}$	-0.08	-0.03
$C_{l, \text{rms}}$	1.13	1.664
$St$	0.102	0.112
Grid points ( $x \times y \times z$ )	120 × 70 × 40	153 × 120 × 32

**Table I.**  
Bulk parameters by grids 1 and 2

observed, the present model captures all major unsteady phenomena unlike the other RANS models which did not capture many features. The results of the present NLKE model are seen to lie in between the experimental data and those predicted by LES computations, showing that the present model is better than the earlier RANS model predictions.

Figure 6 shows the streamwise velocity distribution along the side surfaces of the square cylinder obtained at different stations ( $x/D$ ), by the present computations along with experimental data. The present results match quite well with experimental results, except very near the body where the values are slightly lower. This clearly indicates that the near wall treatment plays an important role and the log-law wall functions are predicting well the magnitude of negative velocities. The improved performance of the log-law functions is due to the inherent assumption that the flow is fully turbulent and applying suitable empirical functions for  $k$  and  $\varepsilon$ . This observation

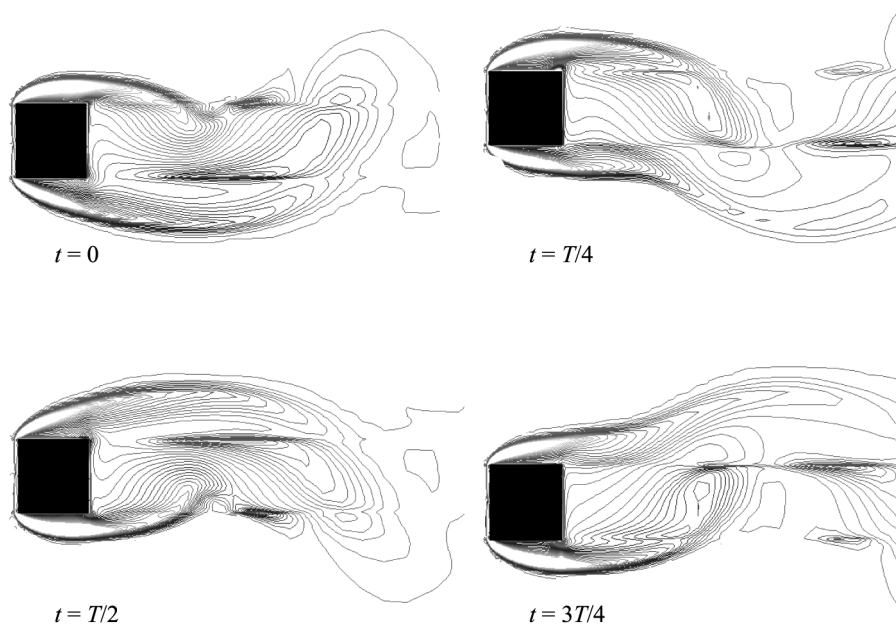


**Figure 4.**  
Iso-vorticity contours at  
different instants of a  
vortex shedding cycle

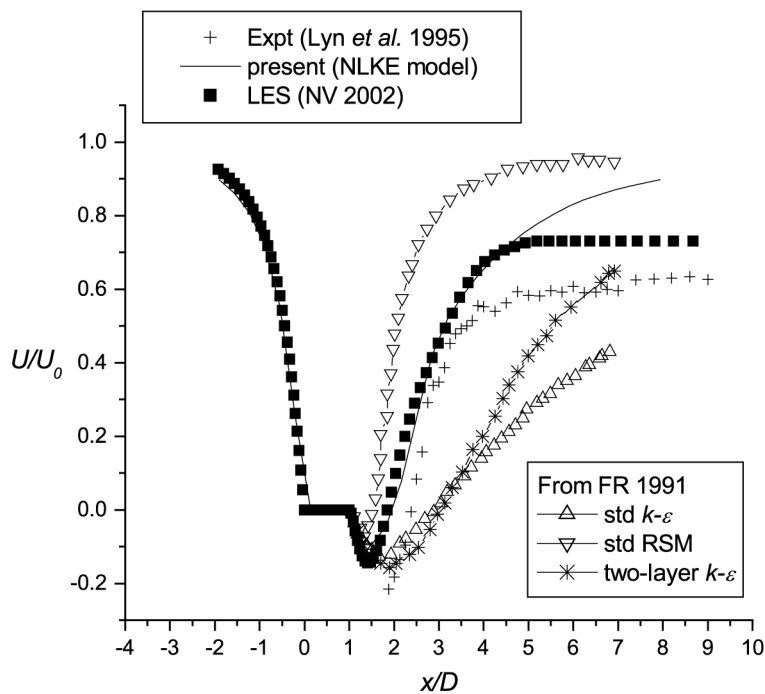


**Figure 5.**  
Mean streamwise velocity  
along the centreline of the  
cylinder



**Table II.**  
Summary of bulk  
parameters for flow over  
square cylinder at  
 $Re = 22,000$

Contribution	Model	$x_r/D$	$C_{d, \text{mean}}$	$C_{d, \text{rms}}$	$C_{l, \text{mean}}$	$C_{l, \text{rms}}$	$St$
Lyn <i>et al.</i> (1995)	Expt.	1.38	2.1	–	–	–	0.132
Lee (1975)	Expt.	–	2.05	0.16–0.23	–	–	–
Rodi <i>et al.</i> (1997)	LES	1.32	2.2	0.14	–	1.01	0.13
Rodi <i>et al.</i> (1997)	RANS	1.25	2.00	–	–	–	0.143
Iaccarino <i>et al.</i> (2003)	Steady RANS	4.81	1.71	–	–	–	–
Iaccarino <i>et al.</i> (2003)	Unsteady RANS	1.45	2.22	0.056	–	1.83	0.141
FR 1991	RSM	0.98	2.250	–	–	–	0.139
FR 1991	Two layer RSM	1.25	2.430	–	–	–	0.143
NV 2002	LES	1.22	2.24	0.118	0.017	1.20	0.136
Present	Unsteady non-linear $k - \epsilon$	1.12	1.89	0.081	–0.03	1.66	0.112

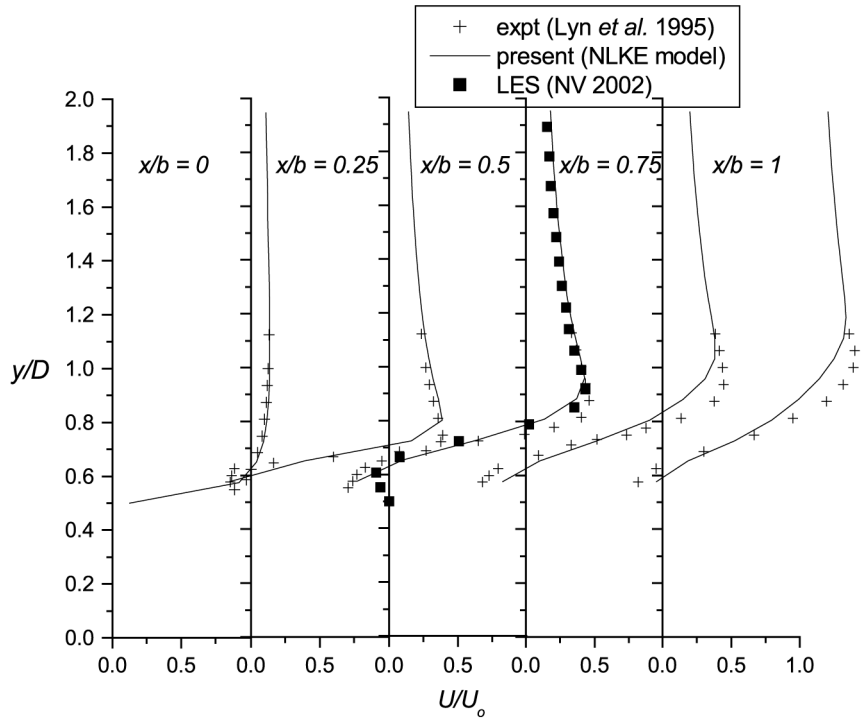


**Figure 6.**  
Mean velocity distribution  
along the side surface of  
the square cylinder

has also been emphasized by Mohamadi and Medic (1996). The mean static pressure ( $C_p$ ) distribution on the surface is shown in Figure 7. On the front and back surface  $C_p$  values are predicted well by the present NLKE model. On the side surface BC or DA, very high suction is predicted at the rear of the body as compared to that of the experiment. These predictions on the side surface are again due to the near wall treatment. The discrepancy in the  $C_p$  distribution on the side surface is also seen in many other LES predictions (Rodi *et al.*, 1997).

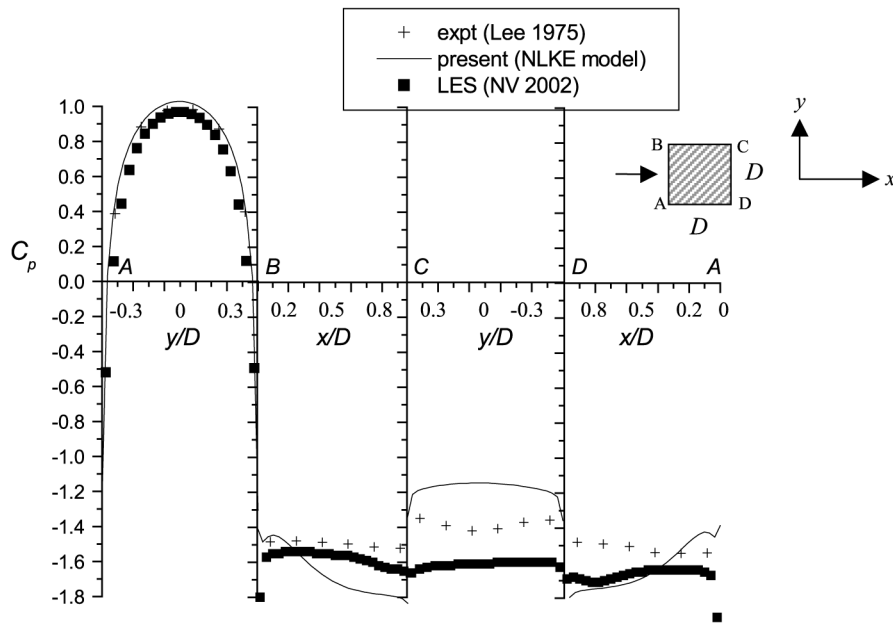


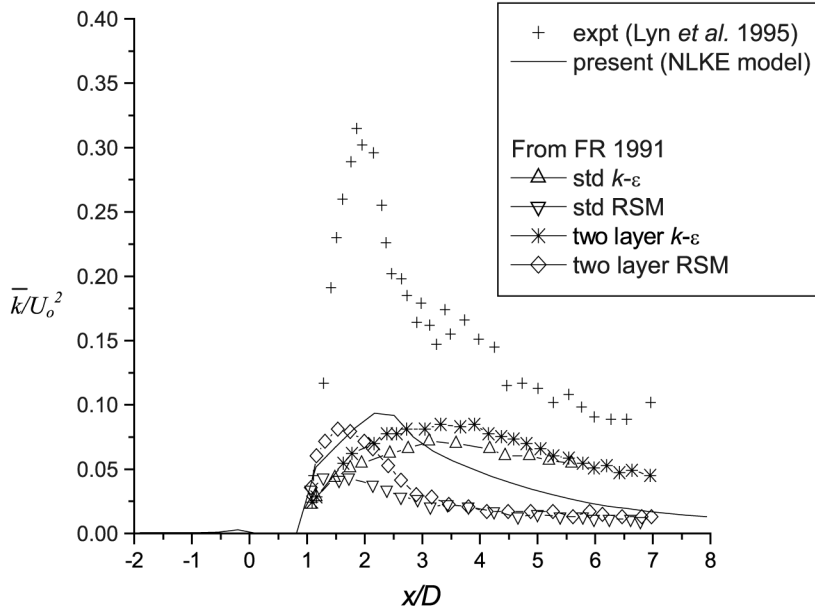
**Figure 7.**  
 $C_p$  distribution on the  
surface of the square  
cylinder

The fluctuating velocity or the rms velocity is obtained when the mean velocity is subtracted from the instantaneous velocity and from this the total fluctuating energy (periodic + turbulent) denoted by  $K_T$  is calculated. The turbulent kinetic energy ( $k$ ) is the modeled or turbulent part and obtained directly by solving the equation. The average of the turbulent kinetic energy,  $\bar{k}$ , and total fluctuating energy,  $\bar{K}_T$ , along the centerline of the cylinder as above are shown plotted against  $x/D$  in Figures 8 and 9, respectively. When compared to the other models, the turbulent kinetic energy is predicted well by the present model. Prediction of the total fluctuating energy by the RSM model matches well with the experimental data, which is probably due to over-prediction of periodic energy. The present model predicts similar to the LES data of Murakami and Mochida (1995), which also under-predicts and this clearly shows that there is no over-prediction of calculated or periodic part by the present model.

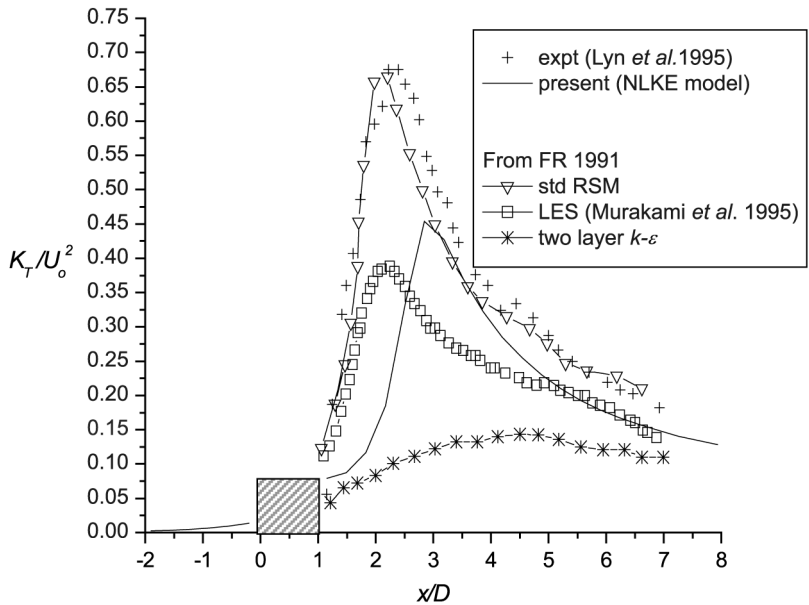
Figure 10 shows the Reynolds stress ( $-\overline{u_1 u_1}$ ) as predicted by the NLKE model with the experimental data of Lyn *et al.* (1995) and LES results of NV 2002. These values are quite close to the experimental values indicating that the model is performing well on the side surface of the cylinder. Figure 11 shows the distributions of turbulent kinetic energy ( $k$ ), and Reynolds stresses ( $-\overline{u_1 u_1}$ ,  $-\overline{u_2 u_2}$ ) on the side surface of the square cylinder as predicted by the present NLKE model. The maximum turbulent kinetic energy increases towards the rear of the cylinder, which is observed to be consistent. It can be also observed from the figure, that as we move away from the cylinder in the wake, the cross-stream Reynolds stress is more predominant than the streamwise Reynolds stress. At  $x/D = 0.25$ ,  $\overline{u_1 u_1}$  is greater than  $\overline{u_2 u_2}$ , whereas at  $x/D = 1$ ,  $\overline{u_2 u_2}$  is larger than  $\overline{u_1 u_1}$ .

The present URANS computation is predicting well the unsteadiness in the flow. It is to be noted that the unsteadiness is partly from the mean flow, i.e. from the vortex

**Figure 8.**  
Comparison of turbulent kinetic energy predicted by different turbulence models with that of experiment



**Figure 9.**  
Comparison of total fluctuating energy predicted by different turbulence models with that of experiment



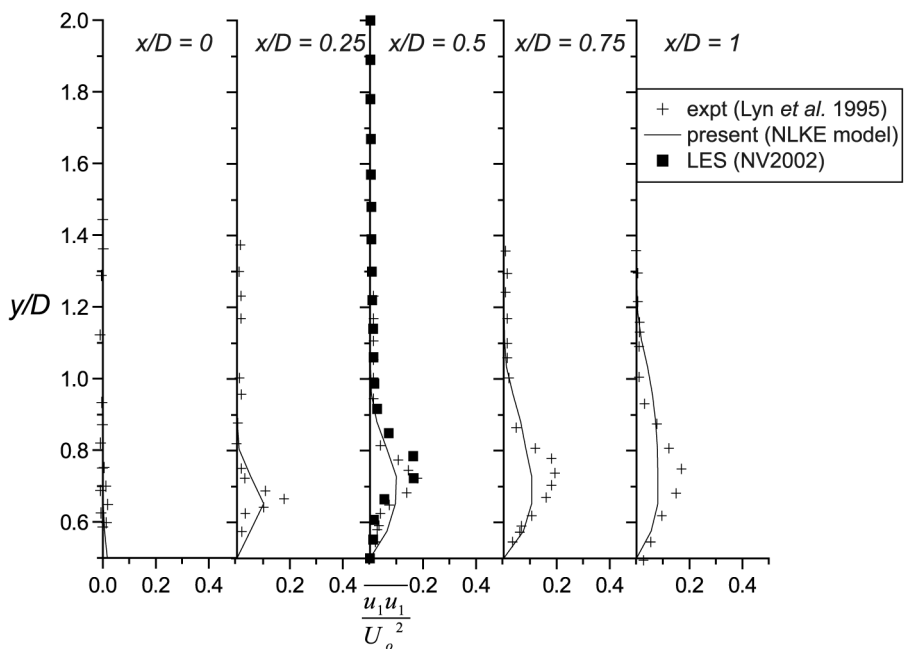


Figure 10.  
 $\overline{u_1 u_1}$  distribution on the side surface of the square cylinder

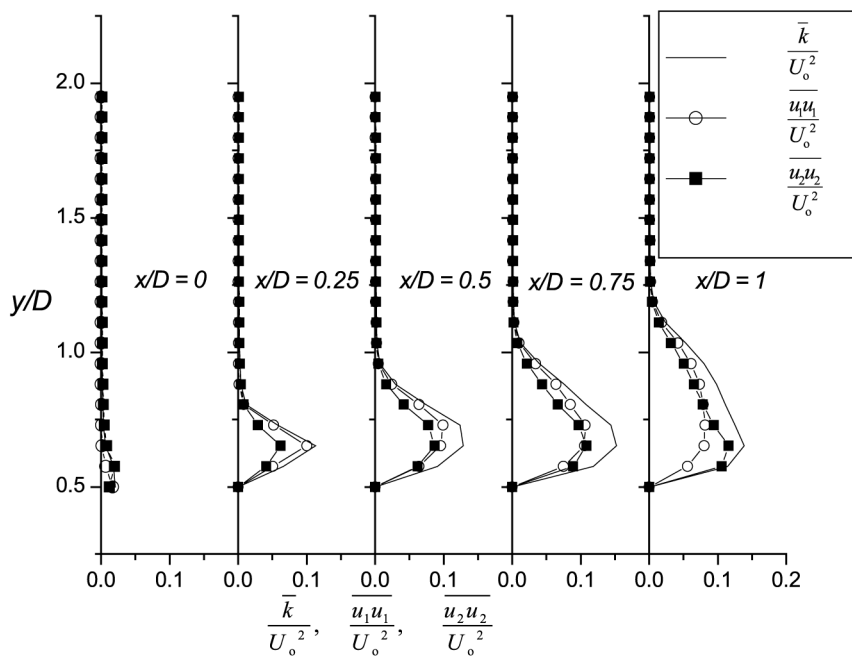


Figure 11.  
 $\bar{k}$ ,  $\overline{u_1 u_1}$ ,  $\overline{u_2 u_2}$  distribution on the side surface of the square cylinder as predicted by the present NLKE model

shedding, and partly due to the turbulence eddies. This can be observed from the proportion of the calculated part of the energy and modeled part of the kinetic energy in the total fluctuating energy. The total fluctuating energy predicted by the present model is of the same order of magnitude as that of LES. This shows that the periodic part of the flow is well calculated by the model. In the present model, the Reynolds stresses are made more dependent on the local rate of strain and vorticity and this is achieved by adding the non-linear terms. The improved prediction of turbulent kinetic energy is obtained by damping the production of  $k$  at the stagnation point by non-linear terms. The  $k$  and  $\varepsilon$  are still used to form the velocity and length scales in the calculation of eddy viscosity. The constant  $C_\mu$  is expressed as a function of local rates of strain and vorticity, which is similar to that in LES, where the sub-grid eddy viscosity is dependent on filter width. It can be said that the unsteadiness produced in the present simulation is due to better prediction of eddy viscosity through modified expression for production terms in transport equations for  $k$  and  $\varepsilon$  and by the functional relation for  $C_\mu$ .

### 5. Conclusion

In the present work, 3D unsteady computation of turbulent flow past a square cylinder is performed. The basic model used is non-linear  $k - \varepsilon$  model. In addition to the comparison with experimental data, the results obtained by the present calculations are compared against available other RANS and LES results. The investigated non-linear  $k - \varepsilon$  model, shows improved predicting capabilities for complex engineering flows by means of an efficient non-linear stress-strain relation and by making the model realizable. Although the results are slightly inferior to that by LES and do not reproduce the same level of agreement with experimental data, the present model captured well all the mean quantities and also the unsteady phenomenon and significantly outperforms that by linear EVM. Performance by the present model can be improved by modeling the coefficients  $\alpha_6$  and  $\alpha_7$  and making the non-linear model a full cubic equation model. On the whole, when comparing the computational time required by the present model and by LES, the accuracy achieved is significant and can be used for simulating 3D unsteady complex engineering flows with reasonable success.

### References

- Craft, T.J., Launder, B.E. and Suga, K. (1996), "Development and applications of a cubic eddy-viscosity model of turbulence", *Int. J. Heat and Fluid Flow*, Vol. 17, pp. 108-15.
- Durbin, P.A. (1995), "Separated flow computations with the  $k - \varepsilon - v^2$  model", *AIAA J.*, Vol. 33, pp. 659-64.
- Franke, R. and Rodi, W. (1991), "Calculation of vortex shedding past a square cylinder with various turbulence models", *In. Proc. of 8th Symposium on Turbulent Shear Flows*, pp. 189-204.
- Gatski, T.B. and Speziale, C.G. (1993), "On explicit algebraic stress models for complex turbulent flows", *J. Fluid Mech.*, Vol. 254, pp. 59-78.
- Iaccarino, G., Ooi, A., Durbin, P.A. and Behnia, M. (2003), "Reynolds averaged simulation of unsteady separated flow", *Int. J. of Heat and Fluid Flow*, Vol. 24, pp. 147-56.
- Kimura, I. and Hosoda, T. (2003), "A non-linear  $k - \varepsilon$  model with realizability for prediction of flows around bluff bodies", *Int. J. Numer. Methods in Fluids*, Vol. 42, pp. 817-37.

- 
- Launder, B.E. and Spalding, D.B. (1974), "The numerical computation of turbulent flows", *Comp. Methods in App. Mech. Engrg.*, Vol. 3, pp. 269-89.
- Lee, B.E. (1975), "The effects of turbulence on the surface field of a square prism", *J. Fluid Mech.*, Vol. 69, pp. 263-82.
- Lyn, D.A., Einav, S., Rodi, W. and Park, J.H. (1995), "A laser Doppler velocimetry study of ensemble-averaged characteristics of the turbulent flow near wake of a square cylinder", *J. Fluid Mech.*, Vol. 304, pp. 285-319.
- Mohamadi, B. and Medic, G. (1996), "A critical evaluation of classical  $k - \epsilon$  model and wall laws for unsteady flows over bluff bodies", *INRIA Report*, 1996.
- Murakami, S. and Mochida, A. (1995), "On turbulent vortex shedding flow past a square cylinder predicted by CFD", *J. Wind Engg. and Ind. Aerodyn.*, Vol. 54, pp. 191-211.
- Nakayama, A. and Miyashita, K. (2001), "URANS simulation of flow over smooth topography", *Int. J. of Numerical Methods in Heat and Fluid Flow*, Vol. 11 No. 8, pp. 723-43.
- Nakayama, A. and Vengadesan, S.N. (2002), "On the influence of numerical schemes and subgrid-stress models on large-eddy simulation of turbulent flow past square cylinder", *Inter. Jl. Numer. Methods Fluids*, Vol. 38 No. 3, pp. 227-53.
- Rodi, W. (1997), "Comparison of LES and RANS calculations of the flow around bluff bodies", *J. Wind Engg. and Ind. Aerodyn.*, Vol. 69-71, pp. 55-75.
- Rodi, W. (2000), "Simulation of turbulence in practical flows", paper presented at European congress on Computational methods in Applied Sciences and Engineering. ECCOMAS 2000.
- Rodi, W., Ferziger, J.H., Breuer, M. and Pourquie, M. (1997), "Status of large eddy simulation: results of a workshop", *Trans. of ASME J. Fluids Engrg.*, Vol. 119, pp. 248-63.
- Shih, T.H., Zhu, J. and Lumley, J.L. (1997), "A new Reynolds stress algebraic equation model", *Comput. Methods Appl. Mech. Engrg.*, Vol. 125, pp. 287-302.

**Corresponding author**

S. Vengadesan can be contacted at: [vengades@iitm.ac.in](mailto:vengades@iitm.ac.in)